

# Plane Pendulum and Beyond by Phase Space Geometry

Bradley Klee<sup>†</sup>

*Department of Physics, University Arkansas, Fayetteville, AR 72701*

(Dated: January 13, 2018)

By careful analysis, the small angle approximation leads to a wildly inaccurate prediction for the period of a simple plane pendulum. We make a perturbation ansatz for the phase space trajectory of a one-dimensional, anharmonic oscillator and apply conservation of energy to set undetermined functions. Iteration of the algorithm yields, to arbitrary precision, a solution to the equations of motion and the period of oscillation. Comparison with Jacobian elliptic functions leads to multi-dimensional applications such as the construction of approximate Seiffert spirals. Throughout we develop a quantum/classical analogy for the purpose of comparing time-independent perturbation theories.

## I. INTRODUCTION

*Space* and *time* play foundational roles in all experiments and most equations. Measurement of space only requires the definition of a standard length. What difficulties prevent easy measurement of time? A day or year is too long for describing the fall of an apple, and heartbeats depend too unpredictably on biological conditions. A pendulum, as in Fig. 1, allows us to set a scale for time on the order of 1 second.

History credits Galileo with the discovery of the pendulum's approximately *isochronous* motion: so long as amplitude of deflection is not too large, the pendulum oscillates with exactly one characteristic time, the period. Whenever the amplitude exceeds a certain range, usually about  $5^\circ$ , the *anisochrony* begins to show as a noticeable increase of period. In general, the timing of a pendulum does depend on its initial condition<sup>1,2</sup>.

After Legendre and Abel, C.G.J. Jacobi standardized the solution of the pendulum's motion by defining a set of elliptic functions<sup>3,4</sup>. The Jacobian elliptic functions have many interpretations in physics, but do not fall into the core curriculum because they present serious technical challenges<sup>5,6</sup>. As an alternative the physics literature contains a variety of approximate methods.

Some authors limit themselves to making a simple yet accurate estimation of the period of oscillation<sup>7,8</sup>. Others attempt to apply the Lindstedt-Poincaré method<sup>1,9,10</sup>. The best available approach seems to be canonical perturbation theory<sup>11</sup>, but this method is couched in language that most physicists will have difficulty understanding. The existing methods leave room for a genuine approach, which arrives at an arbitrary-precision result using a minimal amount of mathematical formalism.

In phase space, solutions to the equations of motion take a geometric form. Periodic motions along one coordinate dimension become closed trajec-

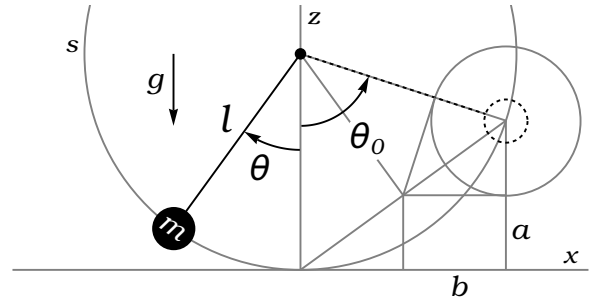


FIG. 1. Simple pendulum and coordinate geometry. Half height  $a$  determines perturbation corrections to the period of the pendulum.

ries, topologically equivalent to circles. We make an ansatz with undetermined functions and apply an iterative algorithm that sets the functions to force convergence of the energy to one conserved value. The solution is a trajectory in phase space, deformed by small perturbations from the  $\mathcal{O}(1)$  elliptical shape.

Comparison with numerical solutions shows that the second approximation suffices to capture the behavior of a pendulum through one period so long as the motion remains constrained to a region  $\theta \in [-\pi/2, \pi/2]$ . By solving the pendulum equations of motion to high precision, we obtain an approximation of the Elliptic functions  $sn(\vartheta, \alpha)$  and  $cn(\vartheta, \alpha)$ . Construction of approximate Seiffert spirals<sup>6</sup> provides proof-of-concept that our approximation methods extend to multi-dimensional problems.

Ultimately we reveal the details of a semiclassical analogy between time-independent perturbation theories. In quantum mechanics approximate wavefunctions must nearly conserve energy. Comparing results for quartic oscillators, we derive a quantum condition, which is equivalent to the Sommerfeld-Wilson prescription in the classical limit.

## II. DIMENSIONAL ANALYSIS

The simple pendulum consists of a massive bob attached by a string or a rod, assumed massless, to an axle as in Fig. 1<sup>2</sup>. Gravity acts on the bob with vertical force  $mg$ , and the attachment applies a response force, the tension. As time elapses the bob swings and executes a periodic motion along a circular trajectory of radius  $l$ . In *librational motion* the pendulum reaches a maximum deflection  $\pm\theta_0$  at regular intervals throughout the experiment. The time of one complete oscillation, say from  $\theta_0$  to  $-\theta_0$  back to  $\theta_0$ , is called the *period*.

Table 1. collects the relevant physical quantities, read directly from Fig. 1. Dimensional symbols  $[L]$ ,  $[M]$ , and  $[T]$ , denote length, mass, and time. First we make a rough estimate of the period,  $T_0$ , by basic dimensional analysis.

**Table 1.** Dimensional Quantities.

Symbol	Dimension	Trigonometric Form
$l$	$[L]$	.
$a$	$[L]$	$l \sin^2(\theta_0/2)$
$b$	$[L]$	$l \sin(\theta_0/2) \cos(\theta_0/2)$
$g$	$[L][T]^{-2}$	.
$m$	$[M]$	.

The quantities  $\{\sqrt{l/g}, \sqrt{a/g}, \sqrt{b/g}\}$  all have dimension of time,  $[T]$ . Assuming Galileo's observation correct,  $\sqrt{l/g}$  must be the dimensional scale of time because quantities  $\{a, b\}$  depend on the amplitude of motion.

A naive energy argument improves the estimation. The maximum potential energy is  $2mga$ . Assume that this energy converts entirely to kinetic energy as the mass  $m$  moves at constant velocity  $2\sqrt{ga}$  through a distance  $8b$ , then  $T_0 \approx 4b/\sqrt{ga}$ . In the small angle approximation,  $a \ll l$ ,  $b \approx \sqrt{l}a$ , and  $T_0 \approx 4\sqrt{l/g}$ . This must be an underestimate mainly because velocity changes between zero and  $2\sqrt{ga}$  throughout the experiment.

The exact period follows from a more sophisticated calculation, again based on conservation of energy. At any height  $z = (l/2)(1 - \cos(\theta)) < a$ , the kinetic energy equals  $2mg(a-z)$ , the velocity equals  $2\sqrt{g(a-z)}$ , and the period equals<sup>1,4</sup>

$$\begin{aligned} T(a/l) &= \int_0^T dt = 4 \int_0^{l\theta_0} \frac{ds}{2\sqrt{g(a-z)}} \quad (1) \\ &= 4\sqrt{\frac{l}{g}} \int_0^{\pi/2} \frac{d\xi}{\sqrt{1-(a/l)\sin^2(\xi)}} = 4\sqrt{\frac{l}{g}} K\left(\frac{a}{l}\right), \end{aligned}$$

where  $ds$  goes along the arc of motion. The complete elliptic integral of the first kind,  $K$ , admits no simple closed-form. Alternatively, the small angle approximation eliminates dependence on  $a$  and

gives a concise result

$$\begin{aligned} T_0 &= \lim_{a \rightarrow 0} 4 \int_0^b \frac{dx}{2\sqrt{g(a-z)}} \quad (2) \\ &= \lim_{a \rightarrow 0} 2\sqrt{\frac{l}{g}} \int_0^a \frac{dz}{\sqrt{z(a-z)}} = 2\pi\sqrt{\frac{l}{g}}, \end{aligned}$$

which requires small-angle identity  $s \approx x \approx 2\sqrt{lz}$  to change from the circular line element  $ds$  to the horizontal  $dx$ , and finally to the vertical  $dz$ . The simple result only applies in the limit  $a \rightarrow 0$ .

In a general one-dimensional oscillation with small-amplitude period  $T_0$ , we usually have something along the lines

$$T(\boldsymbol{\alpha}, \boldsymbol{\epsilon}) = f(\boldsymbol{\alpha}, \boldsymbol{\epsilon}) T_0, \quad (3)$$

with  $f(\boldsymbol{\alpha}, \boldsymbol{\epsilon})$  possibly a complicated function of dimensionless quantities  $\boldsymbol{\alpha}$ , controlled initial conditions of the experiment, and  $\boldsymbol{\epsilon}$ , structure constants of the potential energy.

With the pendulum experiment the trouble is in the initial conditions. Each initial condition determines one critical parameter

$$\alpha = a/l = \frac{1}{2}(1 - \cos(\theta_0)) = \sin^2(\theta_0/2), \quad (4)$$

which we assume proportional to the total energy. In the simple harmonic approximation  $\alpha$  tends to zero as  $\theta_0^2$ . Considering this fact, the hypothesis that factor  $f(\boldsymbol{\alpha}, \boldsymbol{\epsilon}) \rightarrow f(\alpha)$  has a non-terminating power series expansion seems likely. Referencing the expansion of  $K(\alpha)$ <sup>12</sup> we have

$$f(\alpha) = T(\alpha)/T_0 = \frac{2}{\pi} K(\alpha) = 1 + \frac{\alpha}{4} + \frac{9\alpha^2}{64} \dots \quad (5)$$

Numerous approximation schemes (cf.<sup>7</sup>, Table III) aim to simplify the description of a pendulum's *anharmonicity*, as measured by powers of  $\alpha$ . At small  $\alpha$  all formulae for  $T(\alpha)$  must asymptotically approach Eq.5, so exact and approximate agreement to  $\mathcal{O}(\alpha)$  and  $\mathcal{O}(\alpha^2)$  respectively is a common feature of the many published results. For example, the empirical Kidd-Fogg formula<sup>8</sup> has

$$f(\alpha) = \frac{1}{(1-\alpha)^{1/4}} = 1 + \frac{\alpha}{4} + \frac{5\alpha^2}{32} \dots \quad (6)$$

Of course, other factors introduce uncertainty to physical experiments<sup>13</sup>, and these uncertainties always cause the data to deviate from theoretical expectations. Say that we write the standard deviation  $\sigma$  in units of  $T_0$ , then  $\sigma$  competes in order of magnitude with the powers of  $\alpha$  until eventually, for some integer  $n$ , we have  $\alpha^n \ll \sigma$ . This logic gives some restraint to our exploration of approximate solutions.

### III. PENDULUM IN PHASE SPACE

#### A. Small Angle Approximation

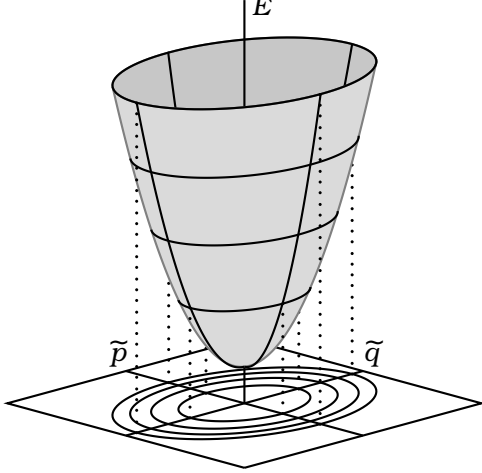


FIG. 2. Total Energy Surface. Level sets of the Hamiltonian energy function project trajectories into the plane of phase space.

In terms of the phase space coordinates,  $(\tilde{q}, \tilde{p}) = (l\theta, ml\dot{\theta})$ , the kinetic and potential energy are

$$T = \tilde{p}^2/2m, \quad V = mgl(1 - \cos(\tilde{q}/l)). \quad (7)$$

The potential function expands in power series

$$V = mgl \sum_{n=1}^{\infty} \frac{(-1)^{n+1}}{(2n)!} (\tilde{q}/l)^{2n}. \quad (8)$$

In the small angle approximation we assume that  $\tilde{q} \ll l$  throughout the experiment. Keeping only the first term allows us to write the conserved, total energy of the pendulum oscillator in the small angle approximation

$$E(\alpha) = 2mgl\alpha \approx \frac{1}{2} \left( \frac{1}{m} \tilde{p}^2 + \frac{mg}{l} \tilde{q}^2 \right). \quad (9)$$

Clearly there exists a bijection between energies and elliptical trajectories, depicted as a projection in Fig. 2. Define radius  $\psi$  and angle  $\phi$  the polar coordinates of phase space. When conservation of energy holds, each trajectory  $\psi(\alpha, \phi) \rightarrow \psi(\alpha)$  is a *time-independent solution* of the equations of motion.

It is much easier to determine time dynamics in a system of measurement where the phase space trajectory takes the particular form of a circle, so we

need to apply a canonical transformation<sup>14</sup>

$$\tilde{q} \rightarrow q = \left( \frac{m^2 g}{l} \right)^{1/4} \tilde{q}, \quad (10a)$$

$$\tilde{p} \rightarrow p = \left( \frac{l}{m^2 g} \right)^{1/4} \tilde{p}, \quad (10b)$$

$$E(\alpha) \rightarrow E(\alpha) = \frac{\omega_0}{2} (p^2 + q^2), \quad (10c)$$

with  $\omega_0 = \sqrt{g/l}$ . Transformation Eq. 10 takes elliptical trajectories into circular trajectories with equal energy and equal enclosed phase area

$$\lambda(\alpha) = \oint d\tilde{q} \tilde{p}(\alpha, \tilde{q}) = \oint dq p(\alpha, q). \quad (11)$$

The period

$$T(\alpha) = \oint dt = \oint d\tilde{q} \frac{m}{\tilde{p}(\alpha, \tilde{q})} = \oint \frac{dq}{\omega_0 p(\alpha, q)}, \quad (12)$$

also remains invariant under the canonical transformation Eq. 10, as we will see shortly.

By applying basic differential geometry to the period integral, it can be shown that the perfect circular shape conserves the "angular momentum" around the origin of phase space, i.e.,  $\dot{\phi} = 0$ . Then the time-dependent solution to the equations of motion is

$$q = \psi(\alpha, 0) \cos(-\omega(\alpha)(t - t_0)) \quad (13a)$$

$$p = \psi(\alpha, 0) \sin(-\omega(\alpha)(t - t_0)) \quad (13b)$$

with angular frequency  $\omega(\alpha) = 2\pi/T(\alpha)$ ,  $t_0$  an arbitrary constant. With  $l\theta_0 \approx 2b$  we have

$$\begin{aligned} \psi(\alpha, 0)^2 &= \left( \frac{m^2 g}{l} \right)^{1/2} (2b)^2 = 4\beta^2 m \sqrt{g l^3} \\ &= 4\alpha(1-\alpha) m \sqrt{g l^3}, \end{aligned} \quad (14)$$

where  $\beta^2 = (b/l)^2 = \alpha(1-\alpha)$ . The constant radius  $\psi(\alpha, 0)$  determines the phase area bounded by closed-curve  $\psi(\alpha)$

$$\begin{aligned} \lambda(\alpha) &= \oint p(\alpha, q) dq = \int_0^{2\pi} d\phi \int_0^{\psi(\alpha, 0)} r dr \\ &= \pi \psi(\alpha, 0)^2 = \lambda_0 (\alpha - \alpha^2), \end{aligned} \quad (15)$$

where  $\lambda_0 = 2mglT_0$ . We have yet to determine  $T(\alpha)$ , and do not assume that  $T(\alpha) = T_0$ . Instead we calculate  $T(\alpha)$  by a beautiful formula<sup>15</sup>

$$T = \frac{d\lambda(\alpha)}{dE(\alpha)} = \oint dq \left( \frac{dE}{dp} \right)^{-1} = \oint \frac{dq}{\omega_0 p}, \quad (16)$$

which proves a connection between the physical period of motion and the purely geometric phase area. As  $\lambda(\alpha)$  and  $E(\alpha)$  remain invariant under canonical transformation so too must  $T(\alpha)$ . Ultimately Eq.

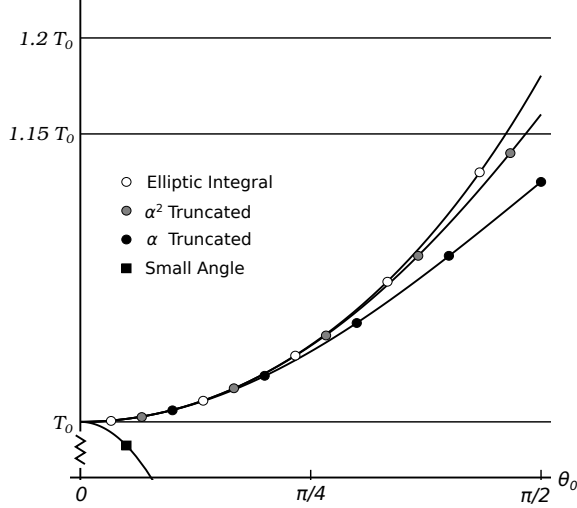


FIG. 3. Comparison of Period Approximations. The small angle approximation obviously diverges away from the exact result obtained by Eq. 1. Truncated curves are  $T_0(1 + \frac{\alpha}{4})$  and  $T_0(1 + \frac{\alpha}{4} + \frac{9\alpha^2}{64})$ .

16 will assuage our delusion and guide us to develop better approximations.

We have defined an entire *phase space geometry*,  $\{E, \psi, \lambda\}$ , in the small angle approximation. Height  $E(\alpha)$  is an exact function of  $\alpha$  while perimeter  $\psi(\alpha)$  and area  $\lambda(\alpha)$  are merely approximations, so we expect to find inconsistency in the geometry wherever the small angle approximation breaks down. Transferring to dimensionless and evaluating Eq. 16 for small angle geometry

$$f(\alpha) = \frac{1}{T_0} \frac{d\alpha}{dE} \frac{d\lambda}{d\alpha} = \frac{1}{\lambda_0} \frac{d\lambda}{d\alpha} = (1 - 2\alpha). \quad (17)$$

Comparing with Eq. 5, we see that  $T(\alpha)$  in the small angle approximation gives the wrong  $\mathcal{O}(\alpha)$  asymptote as depicted in Fig. 3. Worse, the small angle approximation predicts incorrectly that the period *decreases* with increasing total energy!

## B. Simple Anharmonic Approximation

The conclusion of section III.A clearly states the need to find a better approximation of the exact phase space geometry. To present results in a more general fashion, we treat the pendulum as an anharmonic oscillator with a potential  $V$  that expands in power series around a position of stable equilibrium, i.e.,  $\frac{\partial V}{\partial q}|_{q=0} = 0$ ,  $\frac{\partial^2 V}{\partial q^2}|_{q=0} > 0$ . Imposing on potential energy the symmetry constraint  $V(q) = V(-q)$ ,

the most general form for the total energy reduces to

$$E = \frac{\omega_0}{2}(p^2 + q^2) + \sum_{n=1} \frac{\omega_0}{(2(n+1))!} \frac{\epsilon_n}{\lambda_\pi^n} q^{2(n+1)}, \quad (18)$$

We make an ansatz of the form

$$\psi(\alpha, \phi) = \sqrt{2 \lambda_\pi \alpha} \left( 1 + \sum_n \alpha^n \psi_n(\phi) \right), \quad (19)$$

with  $\lambda_\pi = \frac{\lambda_0}{2\pi}$ .

Our strategy is to substitute  $\psi(\alpha, \phi)$  into the energy equation, and determine the functions  $\psi_n(\phi)$  in terms of the expansion coefficients  $\epsilon_n$  by forcing the energy to equal  $\lambda_\pi \omega_0 \alpha + \mathcal{O}(\alpha^{N+2})$  for some integer  $N \geq 0$ . As the phase space trajectory more nearly obeys conservation of energy, the approximation improves.

### 1. $N = 1$ , The $\mathcal{O}(\alpha)$ Approximation

A first approximation only requires the first term of each sum in Eqs. 18 & 19. Applying  $(q, p) \rightarrow (\psi(\alpha, \phi) \cos(\phi), \psi(\alpha, \phi) \sin(\phi))$  to the energy equation and collecting terms by order, we have

$$\alpha : \lambda_\pi \omega_0 \alpha, \quad (20a)$$

$$\alpha^2 : \lambda_\pi \omega_0 \left( \frac{\epsilon_1}{6} \cos^4(\phi) + 2 \psi_1(\phi) \right) \alpha^2. \quad (20b)$$

Setting terms at  $\mathcal{O}(\alpha^2)$  equal to zero and solving for  $\psi_1(\phi)$ , we find

$$\psi(\alpha, \phi) = \sqrt{2 \lambda_\pi \alpha} \left( 1 - \frac{\epsilon_1}{12} \alpha \cos^4(\phi) + \mathcal{O}(\alpha^2) \right). \quad (21)$$

As in section III.A. the phase space geometry determines approximate quantities

$$\begin{aligned} \lambda(\alpha) &= \oint p(\alpha, q) dq = \int_0^{2\pi} d\phi \int_0^{\psi(\alpha, \phi)} r dr \\ &= \lambda_0 \left( \alpha - \frac{\epsilon_1 \alpha^2}{16} \right) + \mathcal{O}(\alpha^3), \end{aligned} \quad (22a)$$

$$f(\alpha) = 1 - \frac{\epsilon_1 \alpha}{8} + \mathcal{O}(\alpha^2). \quad (22b)$$

The pendulum has  $\epsilon_n = (-2)^n$ ,  $\epsilon_1 = -2$ , which makes Eq. 22b asymptotic with Eq. 5 to  $\mathcal{O}(\alpha)$ .

### 2. $N = 2$ , The $\mathcal{O}(\alpha^2)$ Approximation

The approximation improves if we include summands for  $n = 1$  and  $n = 2$ . Evaluation of the energy yields the same constraints as above and

$$\begin{aligned} \alpha^3 : \lambda_\pi \omega_0 \left( \frac{1}{90} \epsilon_2 \cos^6(\phi) + 2 \psi_2(\phi) \right. \\ \left. + \frac{2}{3} \epsilon_1 \cos^4(\phi) \psi_1(\phi) + \psi_1(\phi)^2 \right) \alpha^3. \end{aligned} \quad (23)$$

Setting  $\mathcal{O}(\alpha^3)$  terms equal to zero, substituting the determined form of  $\psi_1(\phi)$ , and solving for  $\psi_2(\phi)$  determines

$$\begin{aligned} \psi(\alpha, \phi) &= \sqrt{2 \lambda_\pi \alpha} (1 - \frac{\epsilon_1}{12} \alpha \cos^4(\phi)) \\ &+ \frac{7 \epsilon_1^2}{288} \alpha^2 \cos^8(\phi) - \frac{\epsilon_2}{180} \alpha^2 \cos^6(\phi) + \mathcal{O}(\alpha^3). \end{aligned} \quad (24)$$

The estimation of  $f(\alpha)$  slightly improves,

$$\begin{aligned} \lambda(\alpha) &= \lambda_0 \left( \alpha - \frac{\epsilon_1 \alpha^2}{16} \right. \\ &\left. + \frac{35 \epsilon_1^2 \alpha^3}{2304} - \frac{\epsilon_2 \alpha^3}{288} \right) + \mathcal{O}(\alpha^4) \end{aligned} \quad (25a)$$

$$\begin{aligned} f(\alpha) &= 1 - \frac{\epsilon_1 \alpha}{8} \\ &+ \frac{35 \epsilon_1^2 \alpha^2}{768} - \frac{\epsilon_2 \alpha^2}{96} + \mathcal{O}(\alpha^3). \end{aligned} \quad (25b)$$

Inserting pendulum values  $(\epsilon_1, \epsilon_2) = (-2, 4)$  makes Eq. 25b asymptotic with Eq. 5 to  $\mathcal{O}(\alpha^2)$ .

### 3. The $\mathcal{O}(\alpha^N)$ Approximation

By iterating the procedure applied for  $N = 1$  and  $N = 2$ , we obtain an approximation to arbitrary order. Every  $\psi_n(\phi)$  can be expanded in Fourier series or in even powers of cosine. When  $\alpha < 1$  the approximation converges according to

$$\lim_{N \rightarrow \infty} E = \lim_{N \rightarrow \infty} \lambda_\pi \omega_0 \alpha + \mathcal{O}(\alpha^{N+2}) = \lambda_\pi \omega_0 \alpha. \quad (26)$$

Clearly convergence depends on  $\alpha$  and becomes slow as  $\alpha$  approaches 1.

Calculation of higher order expansions is a simple routine when written in a language of symbolic computing such as *Mathematica* (Cf. A273506, A273507<sup>16</sup>). An  $N = 10$  approximation computes in less than one second. For moderate ranges of  $\alpha$ , enumeration beyond  $N = 2$  follows a law of diminishing returns. As can be seen in Fig. 3, the  $\mathcal{O}(\alpha^2)$  approximation already captures to within 1%, the exact behavior of the pendulum in the range  $\alpha \in [0, 1/2]$ ,  $\theta_0 \in [-\pi/2, \pi/2]$ .

### C. Time Dependence

The phase space trajectory determines time evolution

$$dt = \frac{dq}{\omega_0 p} = \frac{d\phi}{\omega_0} \left( \frac{\psi'(\alpha, \phi)}{\psi(\alpha, \phi)} \cot(\phi) - 1 \right), \quad (27)$$

where prime indicates differentiation with respect to  $\phi$ . Again expand in powers of  $\alpha$

$$\begin{aligned} \frac{\psi'(\alpha, \phi)}{\psi(\alpha, \phi)} &= \alpha \psi'_1(\phi) + \alpha^2 (\psi'_2(\phi) - \\ &\psi_1(\phi) \psi'_1(\phi)) + \mathcal{O}(\alpha^3), \end{aligned} \quad (28)$$

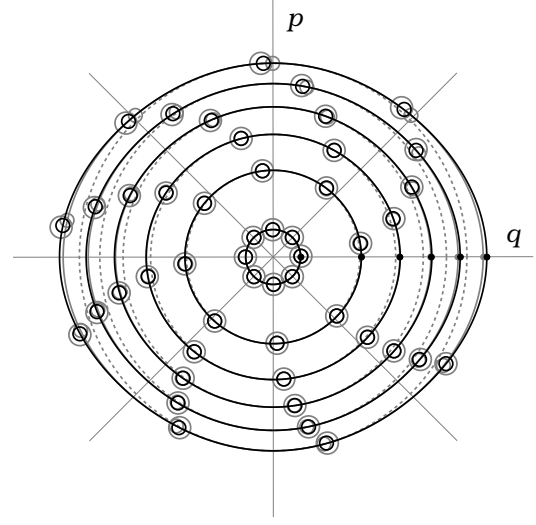


FIG. 4. Time Evolution of Pendulums in Phase Space. The  $N = 2$  ( black ),  $N = 1$  ( gray ), and circular ( dashed gray ) trajectories are plotted for  $\alpha = \{0.01, 0.1, 0.2, 0.3, 0.4, 0.5\}$ . Small filled circles indicate initial conditions, while open circles indicate the state of a system at intervals of  $\Delta t = T_0/8$  as it rotates clockwise through phase space. Large open circles are the prediction of numerical approximation.

Between two near points in phase space

$$\begin{aligned} dt &\approx \frac{d\phi}{\omega_0} \left( -1 + \frac{1}{3} \cos^4(\phi) \epsilon_1 \alpha \right. \\ &\left. + \left( \frac{1}{30} \cos^6(\phi) \epsilon_2 - \frac{1}{6} \cos^8(\phi) \epsilon_1^2 \right) \alpha^2 \right), \end{aligned} \quad (29)$$

where we drop terms higher than  $\mathcal{O}(\alpha^2)$ . Expanding cosine terms (Cf. A273496) allows direct integration of  $dt$ ; however, results at high order are not easy to express in concise form. To first order

$$\begin{aligned} t_1 &= \int_0^{t_1} dt = -\frac{\phi_1}{\omega_0} \left( 1 - \frac{\epsilon_1 \alpha}{8} \right) \\ &+ \frac{\alpha \epsilon_1}{\omega_0} \left( \frac{1}{12} \sin(2\phi_1) + \frac{1}{96} \sin(4\phi_1) \right) + \mathcal{O}(\alpha^2), \end{aligned} \quad (30)$$

with limits  $\phi(0) = 0$  and  $\phi(t_1) = \phi_1$ . By inversion we could in principle obtain  $\phi_1(t_1)$ , but clearly no simple form exists.

Alternatively, we divide space-time line elements and obtain

$$\begin{aligned} \frac{d\phi}{dt} &= \dot{\phi}(\phi) \approx -\omega \left( 1 + \frac{1}{3} \cos^4(\phi) \epsilon_1 \alpha \right. \\ &\left. + \left( \frac{1}{30} \cos^6(\phi) \epsilon_2 - \frac{1}{18} \cos^8(\phi) \epsilon_1^2 \right) \alpha^2 \right). \end{aligned} \quad (31)$$

The phase velocity  $\dot{\phi}$  depends on the phase angle  $\phi$ , as expected in any oscillation where the phase space trajectory deforms away from elliptical or circular

shape. Either limit  $(\epsilon_1, \epsilon_2) \rightarrow (0, 0)$  or  $\alpha \rightarrow 0$  recovers constant  $\dot{\phi}$ , when again trajectories become elliptical.

The determination of  $\dot{\phi}$  for all  $\phi$  allows time-evolution of the approximate symbolic solution, as depicted in Fig. 4. This is the first plot to clearly show anharmonicity as anisochronous motion of pendulums with different initial conditions.

Around  $\alpha = 0$  all approximations become indistinguishable. To  $\alpha = 1/2$ , the  $\mathcal{O}(\alpha)$  approximation closely matches the exact numerical solution, which is nearly indistinguishable from the  $\mathcal{O}(\alpha^2)$  approximation. Isochrony becomes obviously noticeable at high  $\alpha$  where, after 8 intervals of  $\Delta t = T_0/8$ , the pendulum does not nearly reach its initial condition.

#### IV. COMPARISON WITH STANDARDS

##### A. Asymptotic Expansions

Many authors<sup>1,9,10,17,18</sup> attempt to solve anharmonic oscillations using some variant of the Lindstedt-Poincaré method, which essentially applies a least action constraint via the Newtonian equations of motion. This approach is error-prone, and usually a wrong assumption is made regarding time dependence (cf. Eq. 30), which leads to something like  $\psi_1(\phi) = \cos^2(\phi)$ . Taking the wrong  $\psi_1(\phi)$ , it is still possible to compute the correct term of the  $f(\alpha)$  series expansion, so the mistake often escapes notice.

We have already seen in section III.B.1 that in the case of a general quartic oscillator, the first correction to the phase space trajectory is a term like  $\cos^4(\phi)$ , regardless of the magnitude of  $\epsilon_1$ . As opposed to the principle of least action, conservation of energy honestly determines an unambiguous form for the variation functions  $\psi_i(\phi)$ .

##### B. Jacobian Elliptic Functions

The Jacobian elliptic functions determine exactly the phase space geometry of the simple pendulum. The properties of these functions are well known and recorded in a number of resources including Abramowitz & Stegun<sup>19</sup> and Wolfram functions<sup>12</sup>. Paul Erdős gives a creative, geometric introduction via the Seiffert spirals<sup>6</sup>.

The exact pendulum phase space trajectory is

$$q(\alpha, \vartheta) = \sqrt{2 \lambda_\pi} \sin^{-1}(\sqrt{\alpha} \operatorname{sn}(\vartheta, \alpha)), \quad (32a)$$

$$p(\alpha, \vartheta) = \sqrt{2 \lambda_\pi \alpha} \operatorname{cn}(\vartheta, \alpha), \quad (32b)$$

$$\psi(\alpha, \vartheta) = \sqrt{q(\alpha, \vartheta)^2 + p(\alpha, \vartheta)^2}, \quad (32c)$$

where  $\operatorname{cn}$ ,  $\operatorname{sn}$  are Jacobian elliptic functions of angular coordinate  $\vartheta = K(\alpha) + \omega_0 t$  with period  $4K(\alpha)$ .

Substituting in time dependence such as Eq. 30, it is possible to expand  $\psi(\alpha, \vartheta)$  in powers of  $\alpha$  and prove, order-by-order, equivalence between the exact solution and the approximate solution of III.B. We need not perform this tedious calculation, for any solution that conserves energy must be equivalent to the exact solution. Rather, let us explore convergence by plotting the approximations of  $\operatorname{sn}$  and  $\operatorname{cn}$  near the divergence.

Setting the left hand side of Eqs. 32a-b equal to an  $\mathcal{O}(\alpha^N)$  approximation allows us to solve for an approximation of both  $\operatorname{sn}$  and  $\operatorname{cn}$ . Composing approximate trajectories  $\psi(\alpha, \phi)$  and time dependence  $t(\phi)$  gives parametric function graphs appropriately scaled for comparison, as in Fig. 5.

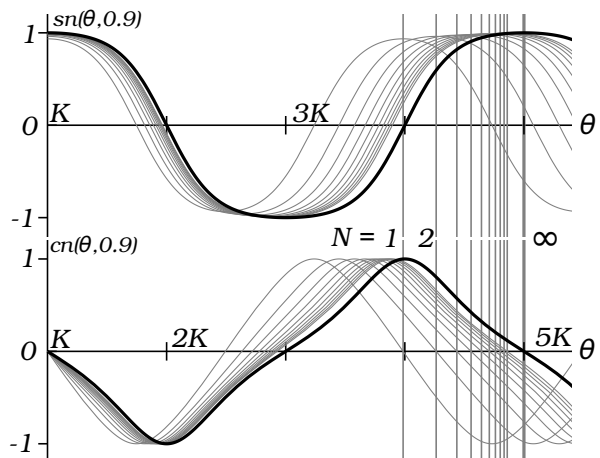


FIG. 5. Approximation Around the Divergence. Approximations of  $\operatorname{sn}$  and  $\operatorname{cn}$  for  $N \in 1, 2, 3, \dots, 10$  are shown to approach the exact functions, even at  $\alpha = 0.9$ . Vertical lines mark the end of one complete period of the  $N^{\text{th}}$  approximation. High values of  $\alpha$  require more terms before the approximation reaches sufficient precision.

Once we extend the approximation to functions such as  $\operatorname{cn}$  and  $\operatorname{sn}$ , it becomes possible to treat other classical motions. Using the inversion relations for elliptical functions<sup>4,6</sup>, we could approximate rotational motion ( $\alpha > 1$ ) of a plane pendulum or solve Euler's equations for the free rotational motion of a rigid body. To perform a more spectacular proof-of-concept, let us partake in Erdős' gedanken.

Our magnanimous goal is to ride a flying machine around Earth on the real space trajectory of a Seiffert spiral<sup>20</sup>, this time *without C.G.J. Jacobi*. A flying machine achieves motion along a *Seiffert spiral* whenever it maintains constant velocity through the air and constant angular velocity around Earth's ro-

tational axis<sup>6</sup>. In theory, a compass and a clock enable navigation whenever we solve for the bearing as a function of time. In practice, a compass and clock navigation system would never work.

The modern world provides a high-precision alternative, namely the Global Positioning System. Let us also assume that the flying machine comes equipped with a GPS unit attached to a simple navigational computer. The trajectory input must be specified as a composition of simple functions such as plus, sine, cosine, power, and sqrt. Then the navigational system outputs either automated control of the vehicle or directions to the pilot.

We take Erdős' equations 2.10 and replace the Jacobian elliptic functions with the approximate solutions described above. The approximate trajectories meet the constraints of the navigational computer, so the computer takes the approximate equations of motion and provides guidance to the craft as it flies the course.

Following Erdős, we choose values of  $\alpha$  that determine closed trajectories. When  $\alpha \ll 1$  even a simple  $N = 1$  approximation allows us to return exactly to the initial condition after, say, going once around the entire world. As shows Fig. 6, whenever  $\alpha$  becomes appreciably large, returning exactly to the initial condition becomes a feat of more precise navigation, i.e., requires input of a trajectory calculated with  $N > 6$ .

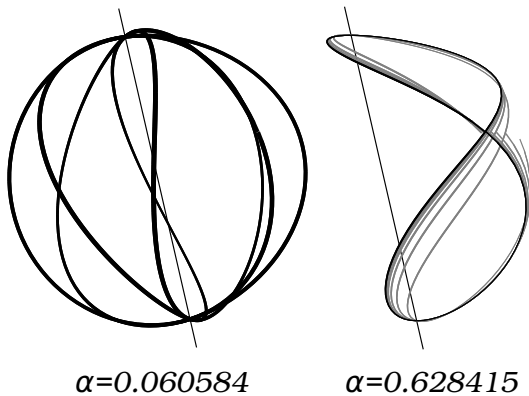


FIG. 6. Approximating Seiffert Spirals. For small  $\alpha$ ,  $N = 1$  approximations closely follow exact Seiffert spirals (left). Approximate trajectories (gray) for  $N = 1, 2, 3, \dots, 6$  approach the exact spiral when  $\alpha \approx 0.628$  (right). The  $N = 7$  approximation (black) appears nearly indistinguishable from the exact spiral.

Comparing Figs. 4, 5, and 6 gives an idea of limitations common to any approximation based on the approximation scheme. In a small angle, even a simple approximation works well. As  $\alpha$  becomes large,

the integrated effect of inexact time-dependence becomes more noticeable, especially after numerous periods of motion. Anisochrony between exact and approximate pendulum solutions becomes positional drift in the navigation experiment.

### C. Canonical Perturbation Theory

The Hamiltonian formulation of mechanics also allows one to obtain an arbitrary-precision expansion for the phase space trajectory by applying a succession of canonical transformations<sup>11</sup>. The method above is similar in spirit but with a gentle learning curve. Moving on to more general calculations may require a stronger Hamiltonian formalism.

## V. QUANTUM CLASSICAL ANALOGY

The choice of nomenclature in section III suggests a quantum/classical analogy at work. The symbol  $\psi$  connotes a quantum wavefunction, but above it denotes a classical phase space trajectory. Our use of  $\psi$  follows other semi-classical works<sup>14,21</sup>. In the sequel, we extend the analogy to time-independent perturbation theory.

### A. Conservation of Energy

Whenever we use approximate methods in the analysis of physical systems, classical or quantum, we also introduce terms of error at some level of precision. For example, approximation of a pendulum's motion may only conserve total energy up to some power of  $\alpha$ . A similar situation often arises in quantum mechanics.

We assume a Hamiltonian  $H = H_0 + \epsilon V$  for which the eigenstates  $|\psi_n\rangle$  are approximately known and non-degenerate,

$$H|\psi_n\rangle = E_n |\psi_n\rangle \quad (33a)$$

$$H_0|\psi_{n,0}\rangle = E_{n,0}|\psi_{n,0}\rangle. \quad (33b)$$

The standard perturbation theory<sup>22</sup> determines corrections to the zero-order wavefunctions and energies.

To first order, the time-independent Schrödinger equation becomes

$$H|\psi_{n,1}\rangle = (E_{n,0} + \epsilon E_{n,1})|\psi_{n,1}\rangle + \mathcal{O}(\epsilon^2). \quad (34)$$

We make the ansatz

$$|\psi_{n,1}\rangle = |\psi_{n,0}\rangle + \sum_{i \neq n} \epsilon c_{n,i}^1 |\psi_{i,0}\rangle, \quad (35)$$

and solve for

$$c_{n,i}^1 = \frac{\langle \psi_{i,0} | V | \psi_{n,0} \rangle}{E_{n,0} - E_{i,0}}, \quad E_{n,1} = \langle \psi_{n,0} | V | \psi_{n,0} \rangle. \quad (36)$$

As with classical perturbation theory, quantum perturbation theory allows iteration to arbitrary  $N$ , where the approximate eigenfunctions

$$|\psi_{n,N}\rangle = |\psi_{n,0}\rangle + \sum_{j=1}^N \sum_{i \neq n} \epsilon^j c_{n,i}^j |\psi_{i,0}\rangle, \quad (37)$$

are nearly stationary with regard to energy

$$H|\psi_{n,N}\rangle = \sum_{i=0}^N \epsilon^i E_{n,i} |\psi_{n,N}\rangle + \mathcal{O}(\epsilon^{N+1}). \quad (38)$$

Though again a law of diminishing returns applies to higher order corrections.

The semiclassical analogy associates conservation of energy with the eigenvalue equation. In either theory, iteration of a recursive algorithm changes the shape of a trajectory or a wavefunction such that the perturbed solution becomes increasingly precise ( Cf. Fig. 7 ).

As time evolves the  $N^{\text{th}}$  classical approximation satisfies

$$\frac{dE}{dt} = 0 + \mathcal{O}(\alpha^{N+2}). \quad (39)$$

To find an analogous equation in quantum dynamics, we apply an infinitesimal time-translation by expanding the Hamiltonian propagator

$$\begin{aligned} |\psi_{n,N}(t + \Delta t)\rangle &= e^{-\frac{i\Delta t}{\hbar} H} |\psi_{n,N}(t)\rangle \quad (40) \\ &\approx (1 - \frac{i\Delta t}{\hbar} H) |\psi_{n,N}(t)\rangle \\ &\approx (1 - \frac{i\Delta t}{\hbar} \sum_{i=0}^N \epsilon^i E_{n,i}) |\psi_{n,N}(t)\rangle + \mathcal{O}(\epsilon^{N+1}). \end{aligned}$$

This equation shows that time-evolution acts on the approximate eigenfunctions as a change of complex phase, but only to  $\mathcal{O}(\epsilon^{N+1})$ . Complex phases cancel in expectation products, so Eq. 40 implies no worse convergence than

$$\frac{d\langle H \rangle}{dt} = 0 + \mathcal{O}(\epsilon^{N+1}). \quad (41)$$

As ever, the analogy involves an obvious fallacy:  $\alpha$  and  $\epsilon$  are dimensionless quantities belonging to two separate classes. In the classical theory, we suppress dependence on the  $\epsilon$  coefficients and assume implicitly that  $\alpha$  can always be chosen to satisfy  $|\alpha \epsilon| \ll 1$  regardless of  $\epsilon$ . The quantum theory requires quantization of  $\alpha$ . After more exploration and explicit calculation, we hope to gain a better understanding of the semiclassical analogy's inner workings.

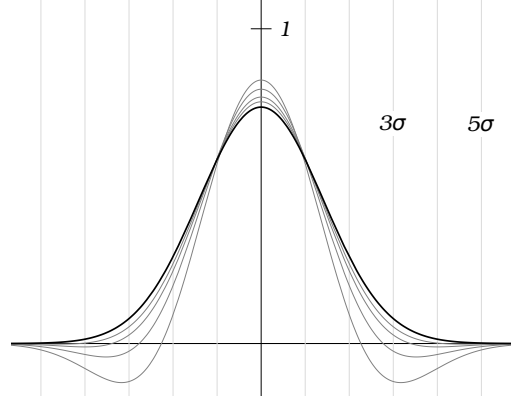


FIG. 7. Perturbed Oscillator Wavefunction. The  $N = 1$  groundstate wavefunctions for Hamiltonian Eq. 42, with  $\epsilon_1 = -2$  and  $(h/\lambda_0) = \{1/2, 1, 2, 4\}$  nearly approach the  $N = 0$  groundstate as  $h/\lambda_0$  becomes small.

## B. Quantum Anharmonic Oscillator

We consider the quantum anharmonic oscillator, with Hamiltonian

$$H = \frac{\omega_0}{2}(p^2 + q^2) + \frac{\omega_0 \epsilon_1}{24 \lambda_\pi} q^4. \quad (42)$$

Using the technique of ladder operators, it is relatively easy to solve for energy to  $\mathcal{O}(\epsilon)$ ,

$$E_{n,0} = \frac{1}{2}(2n + 1)\hbar\omega_0, \quad (43a)$$

$$E_{n,1} = \frac{1}{32}(2n^2 + 2n + 1)\hbar\omega_0, \quad (43b)$$

where  $\hbar = h/(2\pi)$  is the reduced Planck's constant and  $\epsilon = \epsilon_1 \frac{h}{\lambda_0}$ .

Setting equal quantum and classical energies, we see that

$$\begin{aligned} \alpha &= \frac{E_{n,0} + \epsilon E_{n,1}}{\lambda_\pi \omega_0} + \mathcal{O}(\epsilon^2) \quad (44) \\ &= \frac{1}{2} \frac{h}{\lambda_0} (2n + 1) \\ &\quad + \frac{\epsilon_1}{32} \left(\frac{h}{\lambda_0}\right)^2 (2n^2 + 2n + 1) + \mathcal{O}(\epsilon^2), \end{aligned}$$

or equivalently

$$\lambda(n) = (n + \frac{1}{2})h + \frac{\epsilon_1 h^2}{64 \lambda_0} + \mathcal{O}(\epsilon^2). \quad (45)$$

The *quantum conditions* Eqs. 44 & 45 recall the Sommerfeld-Wilson prescription of old quantum mechanics<sup>23,24</sup>

$$\lambda(n) = \oint p dq = n h. \quad (46)$$

Taking the classical limit  $n \rightarrow \infty$ , Eqs. 45 & 46 become equivalent.



In the case of a "quantum pendulum",  $\epsilon_1$  can not be made small, so fidelity of approximate methods depends entirely on the constant  $\lambda_0$ . As  $l$  and  $m$  become increasingly small,  $\lambda_0$  approaches  $h$ . Whenever  $h/\lambda_0 < 1/10$  and  $n < 5$  then  $\alpha < 1/2$ , a first or second approximation adequately describes the quantized trajectories.

## VI. CONCLUSION

The pendulum takes an eminent place in the physics canon, not only as a measurement device but also as an example of anharmonic oscillation. Considering that the simple harmonic approximation fails spectacularly upon careful investigation, we need a better explanation. Here we present a method of analysis that achieves the desired result of arbitrary precision. Calculations require minimal technical skill and by conservation of energy avoid any confusing artifice.

Perturbation methods we apply to the plane pendulum extend beyond this one important example. The ansatz Eq. 19 also solves, to arbitrary order, other parity symmetric potentials. Extending the ansatz to include half-powers of  $\alpha$  allows arbitrary precision solution of any one-dimensional, power-series potential. Furthermore, approximation of the Jacobian elliptic functions provides an entrance to multidimensional problems, as shown by the approx-

imate Seiffert spirals in Section IV.

The classical/quantum analogy reveals fundamental principles that apply throughout physics. Time-independent perturbation theories subject phase space trajectories and wavefunctions to perturbative variations. Evolving through time, trajectories and wavefunctions meet the expectation that higher precision approximations more nearly conserve energy. Exploration of quantum conditions resolves a fallacy in the analogy by showing that quantum theory replaces continuous energy parameter  $\alpha$  with a quantum number  $n$ .

We ultimately reach a detailed understanding of the plane pendulum as a time keeping device. The pendulum is a particular anharmonic oscillator, with a period that varies slightly as a function of amplitude. Moving by analogy to quantum mechanics, we escape anachronism. On the frontiers of modern research, quantum oscillations, for example in Cesium-133, provide the highest precision time scales. Seconds are useful units for time, but in physics we also need milliseconds, nanoseconds, femtoseconds, etc.

## ACKNOWLEDGMENTS

The author gives thanks to Dr. William Harter and Dr. Salvador Barraza-Lopez for many helpful discussions, and comments on an earlier draft of the paper. This work was supported in part by a Doctoral Fellowship awarded by the University of Arkansas.

---

<sup>†</sup> bjklee@email.uark.edu, bradklee@gmail.com

<sup>1</sup> L.D. Landau and E.M. Lifshitz. *Mechanics*. Butterworth-Heinemann, 1976.

<sup>2</sup> W.G. Harter. Classical mechanics with a BANG!, 2016.

<sup>3</sup> C. G. J. Jacobi. *Fundamenta Nova Theoriae Functionum Ellipticarum*. Königsberg, 1829.

<sup>4</sup> John Vernon Armitage and William Frederick Eberlein. *Elliptic functions*, volume 67. Cambridge University Press, 2006.

<sup>5</sup> Thomas E. Baker and Andreas Bill. Jacobi elliptic functions and the complete solution to the bead on the hoop problem. *American Journal of Physics*, 80(6):506–514, 2012.

<sup>6</sup> Paul Erdős. Spiraling the earth with c.g.j. jacobi. *American Journal of Physics*, 68(10):888–895, 2000.

<sup>7</sup> Claudio G. Carvalhaes and Patrick Suppes. Approximations for the period of the simple pendulum based on the arithmetic-geometric mean. *American Journal of Physics*, 76(12):1150–1154, 2008.

<sup>8</sup> Richard B. Kidd and Stuart L. Fogg. A simple formula for the large-angle pendulum period. *The Physics Teacher*, 40(2):81–83, 2002.

<sup>9</sup> E.J. Hinch. *Perturbation Methods*. Cambridge Texts in Applied Mathematics. Cambridge University Press, 1991.

<sup>10</sup> A.H. Nayfeh. *Perturbation Methods*. Wiley, 2008.

<sup>11</sup> J.H. Lowenstein. *Essentials of Hamiltonian Dynamics*. Cambridge University Press, 2012.

<sup>12</sup> Wolfram Research. Wolfram functions: Elliptic functions, 2016.

<sup>13</sup> Robert A. Nelson and M.G. Olsson. The pendulum-rich physics from a simple system. *American Journal of Physics*, 54(2):112–121, 1986.

<sup>14</sup> John P. Ralston. Berry's phase and the symplectic character of quantum time evolution. *Physical Review A*, 40(9):4872, 1989.

<sup>15</sup> V.I. Arnold. *Mathematical Methods of Classical Mechanics*. Graduate Texts in Mathematics. Springer New York, 2013.

<sup>16</sup> Neil J.A. Sloane et al. The on-line encyclopedia of integer sequences, 2016.

<sup>17</sup> Lewis P. Fulcher and Brian F. Davis. Theoretical and experimental study of the motion of the simple pendulum. *American Journal of Physics*, 44(1):51–55, 1976.

- <sup>18</sup> D. Park. *Classical Dynamics and Its Quantum Analogues*. Springer New York, 2012.
- <sup>19</sup> Milton Abramowitz and Irene A. Stegun. *Handbook of mathematical functions*, volume 55. Courier Corporation, 1964.
- <sup>20</sup> Alfred Seiffert. *Über eine neue geometrische Einführung in die Theorie der elliptischen Funktionen*. Wissenschaftliche Beilage zum Jahresbericht der Städtischen Realschule zu Charlottenburg, Ostern, 1896.
- <sup>21</sup> William G. Harter. Su(2) coordinate geometry for semiclassical theory of rotors and oscillators. *The Journal of chemical physics*, 85(10):5560–5574, 1986.
- <sup>22</sup> P.J.E. Peebles. *Quantum Mechanics*. Princeton University Press, 1992.
- <sup>23</sup> S. Tomonaga. *Quantum Mechanics: I, Old quantum theory*. North-Holland, 1968.
- <sup>24</sup> M.S. Child. *Semiclassical mechanics with molecular applications*. Clarendon Press, Oxford, 2014.